




Article

Outdoor Thermal Comfort Optimization in a Cold Climate to Mitigate the Level of Urban Heat Island in an Urban Area

Nasim Eslamirad ^{1,*}, Abel Sepúlveda ^{2,3} , Francesco De Luca ³ , Kimmo Sakari Lylykangas ³ 
and Sadok Ben Yahia ⁴

¹ FinEst Centre for Smart Cities, Tallinn University of Technology, 10115 Tallinn, Estonia

² Architecture and Intelligent Living, Karlsruhe Institute of Technology, 76131 Karlsruhe, Germany; abel.luque@taltech.ee

³ Department of Civil Engineering and Architecture, Tallinn University of Technology, 10115 Tallinn, Estonia; francesco.deluca@taltech.ee (F.D.L.); kimmo.lylykangas@taltech.ee (K.S.L.)

⁴ Department of Software Science, Tallinn University of Technology, 10115 Tallinn, Estonia; sadok.ben@taltech.ee

* Correspondence: nasim.eslamirad@taltech.ee

Abstract: Climatic and micro-climatic phenomena such as summer heat waves and Urban Heat Island (UHI) are increasingly endangering the city's livability and safety. The importance of urban features on the UHI effect encourages us to consider the configuration of urban elements to improve cities' sustainability and livability. Most solutions are viable when a city redevelops and new areas are built to focus on aspects such as optimum design and the orientation of building masses and streets, which affect thermal comfort. This research looks beyond outdoor thermal comfort studies using UHI data and geoprocessing techniques in Tallinn, Estonia. This study supposes that designing urban canyons with proper orientation helps to mitigate the UHI effect by maximizing outdoor thermal comfort at the pedestrian level during hot summer days. In addition, optimizing the orientation of buildings makes it possible to create shaded and cooler areas for pedestrians, reducing surface temperature, which may create more comfortable and sustainable urban environments with lower energy demands and reduced heat-related health risks. This research aims to generate valuable insights into how urban environments can be designed and configured to improve sustainability, livability, and outdoor thermal comfort for pedestrians. According to the study results, researchers can identify the most effective interventions to achieve these objectives by leveraging UHI data and geoprocessing techniques and using CFD simulations. This evaluation is beneficial in guiding urban planners and architects in proposing mitigation solutions to enhance thermal comfort in cities and creating suitable conditions for approved thermal comfort levels. Results of the study show that in the location used for the survey, Tallinn, Estonia, the orientation of West-East offers the optimum level of comfort regarding thermal comfort and surface temperature in the urban environment.

Keywords: urban climate changes; outdoor thermal comfort; Urban Heat Island (UHI); surface temperature; mitigation strategies of UHI effect



Citation: Eslamirad, N.; Sepúlveda, A.; De Luca, F.; Sakari Lylykangas, K.; Ben Yahia, S. Outdoor Thermal Comfort Optimization in a Cold Climate to Mitigate the Level of Urban Heat Island in an Urban Area. *Energies* **2023**, *16*, 4546. <https://doi.org/10.3390/en16124546>

Academic Editors: Vincenzo Costanzo and Korjenic Azra

Received: 19 April 2023

Revised: 1 June 2023

Accepted: 2 June 2023

Published: 6 June 2023



Copyright: © 2023 by the authors. Licensee MDPI, Basel, Switzerland. This article is an open access article distributed under the terms and conditions of the Creative Commons Attribution (CC BY) license (<https://creativecommons.org/licenses/by/4.0/>).

1. Introduction

According to the European Environment Agency (EEA) [1], the number of megacities has nearly tripled since 1990 [2]. Recognizing the paramount importance of providing secure, healthy, and comfortable housing for individuals' overall well-being, urban design plays a critical role in mitigating the adverse effects of climate change on cities [2]. The rapid expansion of urban areas brings about significant alterations in surface temperatures, particularly in densely populated regions characterized by impermeable surfaces that absorb substantial solar radiation, resulting in heat retention within buildings [3]. By effectively managing the factors that influence the urban microclimate, the quality of life

for city residents can be significantly improved [2]. Conversely, inadequate urban design exacerbates the impacts of climate change in urban areas [1].

The UHI effect is a specific phenomenon associated with urban environments, leading to substantially higher temperatures than surrounding rural areas [2]. UHI contributes to a 2–5 °C temperature rise in urban areas [3]. The low level of thermal comfort in cities emphasizes the urgent need for urban planners to prioritize sustainability and reevaluate their approaches. This is particularly significant due to the far-reaching impacts of urban warming on health, well-being, human comfort, and the local atmosphere [4,5], as well as the economic and social systems of cities [1]. Brian Stone highlighted in 2012 that major cities worldwide are experiencing temperature increases faster than the rest of the planet [6].

Consequently, there is a pressing need to present mitigation strategies to address the exponential growth of UHI and heat waves associated with rising urban temperatures. As a result, scientific interest in mitigating UHI has increased, reflecting an increased awareness among scientists, urban planners, and governmental organizations [7,8]. This is primarily due to UHI's direct impact on urban residents' health [4,9] and its implications for their well-being, human comfort, and the local atmosphere [8].

Research on the UHI phenomena often focuses on the canopy layer and investigates it at micro and local scales, such as single-street canyons and neighborhoods [10]. The design configuration of urban areas, including optimized building and street geometry and orientation, plays a crucial role in influencing solar radiation and airflow within an urban canyon [11]. Among the various measures used to assess UHI, ambient temperatures, including air and surface temperatures, are particularly important [4]. In urban street canyons, the amount of solar radiation directly impacts solar access and, consequently, the thermal comfort experienced by pedestrians [11]. Hence, incorporating these strategies into urban development plans could create more sustainable, resilient, and livable cities [12].

However, there are still limitations in studies concerning outdoor thermal comfort, mainly due to the inefficiency of simulations and the challenge of applying assessment results during the early stages of the design process [13]. Furthermore, UHI mitigation strategies still face several hurdles, such as the complexity of execution and the difficulty in effectively communicating scientific knowledge to municipal governments and urban planners [7].

While various strategies for mitigating the UHI effect have been acknowledged, there is still a need to bridge the gap between the accumulated knowledge and the practical implementation of UHI mitigation measures. One approach to address this is to consider the influence of outdoor comfort levels and surface temperatures during the design process of urban elements and building extensions. Furthermore, Computational Fluid Dynamics (CFD) and numerical simulations allow researchers to assess design scenarios and compare their effectiveness in mitigating UHI and improving outdoor thermal comfort in urban areas.

Furthermore, rather than retrofitting existing urban areas, it is advantageous to incorporate UHI mitigation strategies right from the start when developing new cities. Since thermal comfort is a crucial factor in design considerations [14], analyzing the geometry and orientation of urban canyons and surrounding buildings enables researchers to determine the optimal configuration that maximizes shading, airflow, and solar radiation. This optimization approach helps minimize the UHI effect and enhance outdoor thermal comfort.

This study offers a unique contribution through its innovative approach of sampling urban areas using geoprocessed urban data. It extensively analyzes the relationship between building orientation, outdoor thermal comfort, urban surface temperature, and the UHI effect, specifically in Tallinn, Estonia. Additionally, the study introduces a novel method for analyzing the Physiological Equivalent Temperature (PET) value, utilizing a scaling evaluation method. This study provides a valuable opportunity to gain insights into the intricate interplay between urban features, microclimate conditions, and human well-being through the implementation of optimization research. The findings obtained

from this research can inform and guide decision-making processes in urban design and planning. This study offers valuable insights that can contribute to developing informed and effective strategies for mitigating the UHI effect. By incorporating these insights, urban planners, architects, and policymakers can make informed decisions and create design guidelines that promote sustainable and livable urban environments.

The essence of this research as an optimization urban research has three main objectives:

Objective 1: To evaluate the outdoor thermal comfort at the pedestrian level in different scenarios of building mass orientation in the urban canyon. This objective holds significance as it directly impacts the well-being of city residents and aids in identifying the most favorable and sustainable design solutions for residential areas.

Objective 2: To evaluate the surface temperature of different building mass orientation scenarios. Surface temperature plays a pivotal role in the UHI effect, and comprehending its behavior in different scenarios is essential for identifying effective UHI mitigation strategies and making informed design decisions.

Objective 3: To propose solutions that improve the quality of life regarding outdoor thermal comfort to help reduce the effect of UHI in Tallinn. This objective holds great importance in light of the growing significance of urbanization and climate change as global concerns.

After the Introduction, the paper is divided into five sections:

Section 2 provides an overview of the literature review and related works based on an extensive review of published academic research studies. Section 3 discusses the material and methods applied in the study. Section 4 presents the numerical analysis and CFD simulation to assess the outdoor thermal comfort and surface temperature of case studies in different scenarios. Section 5 is related to the assessment results. The discussion follows in the next section with the interpretation of the results and the study's conclusion.

2. Background

2.1. UHI Effect and Surface Temperature Studies

Rapid global urbanization has resulted in extensive urban development, with a significant portion of the global population residing in cities. This trend is projected to increase to around five billion people, or 61 percent of the global population, by 2030 [2]. In Europe, the percentage of the population living in cities is currently around 73%, with an expected rise to 82% [1]. Due to urbanization and global climate change, urban areas experience higher temperatures than non-urban regions. This trend is expected to continue throughout the 21st century, leading to higher temperatures in urban areas than in non-urban regions due to the UHI phenomenon [15]. The phenomenon of UHI resulting from urbanization was first observed in 1818 by Howard [5]. The occurrence of heatwaves and the UHI effect presents significant climate risks to cities, leading to extensive research efforts to explore various methods to mitigate their impacts [6]. The intensity of the UHI is a measure of the additional heat introduced into the atmosphere by urban areas [16]. Changes in the urban thermal environment substantially impact the energy balance within urban areas, affecting boundary meteorology and climatology [3]. These factors have socio-economic implications, including increased energy consumption, heightened vulnerability to heat-related illnesses, and higher mortality rates [17]. Consequently, it is essential to investigate UHI mitigation strategies sustainably [4]. Accurate analysis and understanding of UHI's spatial and temporal variations of UHI are crucial for effective management and mitigation efforts [17].

Mitigating the UHI phenomenon through physical environmental modifications is crucial for altering the urban microclimate. Implementing large-scale mitigation measures encompassing the entire urban environment can significantly impact the urban microclimate [7]. The research conducted by Akbari, Rosenfeld, and Taha at the Lawrence Berkeley National Laboratory played a crucial role in popularizing the concept of UHI mitigation [7]. UHI mitigation is essential for improving human thermal comfort and creating better living environments in urban residential areas. However, limited attention has been given to understanding the combined effects of UHI mitigation strategies on human thermal

comfort [18]. Akbari suggests various strategies to reduce UHI and enhance thermal comfort in cities, highlighting that the intensity of UHI is influenced by urban characteristics, micro-climatic conditions, urban materials, and green spaces within urban areas [1]. The arrangement of buildings and the land's topography play crucial roles in determining temperature distribution within a city [19]. Additionally, urban geometry plays a pivotal role in controlling the retention and release of heat, emphasizing its significance in the UHI phenomenon. Therefore, it is vital to understand how urban geometry influences these factors to implement effective strategies for UHI mitigation [17].

In 2009, Giguère compiled a comprehensive inventory of UHI mitigation strategies, categorizing them into four groups. These categories include vegetation and cooling measures such as selective tree planting, greening of parking lots, and implementing green roofs. The second category is sustainable urban infrastructure, focusing on designing buildings and roads with UHI mitigation in mind. Third, sustainable water management is another category that utilizes trees, green roofs, permeable surfaces, and retention ponds to manage water in urban areas. Lastly, reducing anthropogenic heat involves controlling heat production, reducing vehicle numbers, and implementing efficient air conditioning systems [7].

Dynamic numerical approaches are the most reliable and satisfactory method for assessing the effectiveness of UHI mitigation strategies [5]. Similarly, in a study conducted in Toronto, various UHI mitigation strategies were evaluated in different urban neighborhoods using numerical simulations with the ENVI-met software to gauge their impact on reducing UHI effects. The study revealed that urban form significantly influences the duration of direct sun and mean radiant temperature, which are crucial factors in determining urban thermal comfort [20].

In a study conducted in the Sydney metropolitan area, researchers examined the impact of various urban design factors on ambient and surface temperatures in open spaces. Factors such as building height, street width, aspect ratio, built area ratio, orientation, and dimensions of open spaces were analyzed. Using the ENVI-met simulation tool, the study developed fourteen precincts to simulate different scenarios, both with and without mitigation measures. The results demonstrated a strong correlation between the gradient of temperature decrease along the precinct axis (GTD) and the average aspect ratio of the precincts, regardless of whether mitigation strategies were implemented. As a result, the study suggests that implementing urban design interventions that modify the aspect ratio of buildings and streets can effectively mitigate the UHI effect and improve thermal comfort in open spaces [21].

Additionally, Xu et al. conducted a study investigating the potential of using the spatial equity of green areas in cities and land surface temperature to mitigate UHI effects. Their findings indicated that increasing the amount of urban green spaces can be beneficial in reducing the average urban temperature and mitigating UHI effects [22]. Similarly, another study focused on improving UHI in Mandaue, Philippines, through various mitigation measures, including increasing vegetation, adding open spaces, employing green roofs, and combining these strategies. The study considered changes in air temperature, surface temperature, and thermal comfort in the study areas to understand the impact of altering green areas and implementing green roofs on reducing the UHI effect [23].

Using ENVI-met simulations, another study investigates how the built environment impacts microclimate parameters. It confirms the existence of the UHI phenomenon in Chennai, India, emphasizing the importance of urban planning in designing neighborhoods that prioritize thermally comfortable outdoor spaces to enhance pedestrian comfort. These findings have significant implications for urban planners, underscoring the need to consider thermal comfort when designing outdoor areas [24]. Similarly, the study explores the influence of urban form parameters on pedestrian thermal comfort in the arid climate of Mashhad, Iran. By employing the ENVI-met software, the researchers analyze these parameters to predict outdoor thermal comfort conditions in current and future urban contexts. To assess outdoor thermal comfort, the study proposes an alternative approach for cities,

advocating using UHI zoning to replace traditional urban form zoning. This alternative method proves particularly advantageous in large cities where gathering data on the urban form is challenging due to limited resources and time constraints. By incorporating UHI zoning, urban planners can effectively evaluate and enhance outdoor thermal comfort in urban areas [25].

In another study focusing on hot climate conditions, Farhadi et al. assessed various strategies for mitigating the UHI effect and improving thermal comfort in Tehran, which experiences urban warming. Their findings revealed a strong correlation between lower surface temperatures and the reduction of the UHI effect, leading to improved thermal comfort [26]. Similarly, Arnfield's research indicated that the orientation of streets plays a significant role in determining the amount of solar energy absorbed by walls [27]. Likewise, Van Esch et al. examined the effects of street width and orientation, as well as building parameters such as roof shape and building envelope, on solar access to the urban canopy and the viability of passive solar heating strategies in residential buildings [28]. Furthermore, evaluations of the UHI effect in numerous cities and villages across the Netherlands demonstrated a significant UHI in most Dutch cities. The 95th percentile of the UHI is strongly correlated with population density [29]. Additionally, the design of streets, the orientation of urban canyons, and the presence of trees had a remarkable impact on ground surface temperatures and outdoor thermal comfort, consequently influencing the UHI effect [30].

2.2. Outdoor Thermal Comfort Studies

The potential for reducing outdoor air temperatures in a square in Rome was studied using a numerical model created using the ENVI met tool to simulate different mitigation scenarios to reduce warming in urban areas. The study found solutions such as using grass pavers to provide the most significant advantages that could enhance the thermal conditions of the air and reduce outdoor air temperatures [31].

Fazia Ali-Toudert et al. discuss the role of street design, such as aspect ratio, and orientation, towards developing pedestrian-level comfortability. The study benefits of the three-dimensional numerical model ENVI-met, simulating microclimatic changes within urban environments in a high spatial and temporal resolution in Ghardaia, Algeria. The study analyzed the symmetrical urban canyons with various height-to-width ratios and different solar orientations (i.e., East–West, North–South, North East–South West, and North West–South East). In addition, the study assessed outdoor thermal comfort value in the physiologically equivalent temperature (PET) index. The results show contrasting patterns of thermal comfort between shallow and deep urban streets and the various orientations. Moreover, the results prove that PET at the street level depends strongly on aspect ratio and street orientation [32]. Another study evaluated the potential for UHI mitigation of greening parking lots and the relationships between land surface temperature (LST) and land use/land cover (LULC) in different seasons in Nagoya. The results show that different LULC types play different roles in different seasons and times, and using more green areas slightly reduced the LST for the whole study area in spring or summer [3]. The other study that used qualitative and quantitative approaches to assess outdoor thermal comfort as a mixed method identified which urban areas need more improvement during the summer. The results of thermal comfort assessment through the PET index and subjectively perceived thermal sensation using ENVI-met environment to do CFD simulation and thermal comfort assessment [33].

In the study by Giridharan, the author defines urban compactness as a combination of various urban design factors, including the building area-to-volume ratio, aspect ratio (height to width), sky view factor, distance to the nearest wall, width of the street, built-up area, green areas, albedo, water surface size, roads, open areas, and distance to a heat sink [10]. These factors influence the urban microclimate, and their combination can affect the level of UHI and outdoor thermal comfort in urban areas. In addition, Aleksandrowicz et al. outline the physical features of the urban environment, such as the

density of buildings, the area of land used and unoccupied areas, and the type of materials in urban components, which all affect UHI level and strength [7].

The background studies and literature review show that heat waves and the UHI effect are significant climate risks affecting cities. There are many ways in which urban design can be modified to mitigate the UHI effect in cities, such as increasing green spaces, using reflective or high albedo materials, modifying the built environment, reducing the anthropogenic heat, and optimizing building and urban canopy orientation and layout. These modifications can help decrease surface temperatures in urban areas, which can significantly impact the UHI effect and the level of thermal comfort experienced by people living and working in these environments. Additionally, by evaluating the orientation and extension of buildings and urban canyons that affect the amount of solar radiation, which impacts local temperatures and, consequently, the surface temperature and thermal sensation in the urban area, we can help to lower temperatures and improve thermal comfort at the pedestrian level, the surface temperature in the urban canyon, and UHI effect in the urban area during hot summer days. Furthermore, these modifications can also provide other benefits, such as enhancing the comfort and livability of urban areas and creating more sustainable and resilient environments that promote the health and well-being of all residents. The study's findings will be valuable to urban planners and designers as they influence decisions about designing and configuring urban elements to create more sustainable and comfortable environments.

2.3. Novelty of This Investigation

The literature review highlights the significant influence of city layout and structure on heat waves and the UHI effect. Previous research emphasizes dynamic numerical approaches to assess UHI, outdoor thermal comfort, and surface temperatures, enabling the identification of mitigation strategies.

This study suggests designing urban canyons with proper orientation as an effective method to mitigate the UHI effect and enhance pedestrian comfort during hot summer days. Optimizing building orientation creates shaded and cooler areas, reducing surface temperatures and heat concentration. This approach promotes more sustainable urban environments with lower energy demands and decreased health risks.

The study's novelty lies in the innovative sampling technique using geoprocessed UHI urban data from Tallinn. Extensive numerical analysis establishes the relationship between building orientation, outdoor thermal comfort, urban surface temperature, and the UHI effect. In addition, a new method for analyzing the Physiological Equivalent Temperature (PET) value is introduced. By prioritizing resident well-being, addressing heat waves, and proposing UHI mitigation strategies, this research contributes to the development of livable and sustainable urban spaces.

3. Methodology

Using three specific case studies, we examined the space between a target building and its nearest neighboring building across the street. Each case study involved a geometric model of an actual residential building in Tallinn, including the urban canopy, the nearby neighbor building(s), and the street in between. These case studies aimed to determine the optimal orientation of the building mass that would ensure the highest level of outdoor thermal comfort and the lowest surface temperature in the analyzed area during hot summer days.

The building direction often describes the orientation of the canyon axis (e.g., North–South, East–West) or (North West–South East, North East–South West) [2]. In the definition of scenarios and the simulated models of the study, the orientation of the canyon axis represents the direction of an elongated space, measured (in degrees) as the angle between a line running North–South and a significant axis running the length of a street or other linear area, measured counterclockwise. Figure 1 shows mentioned orientations on the axis of four main directions.

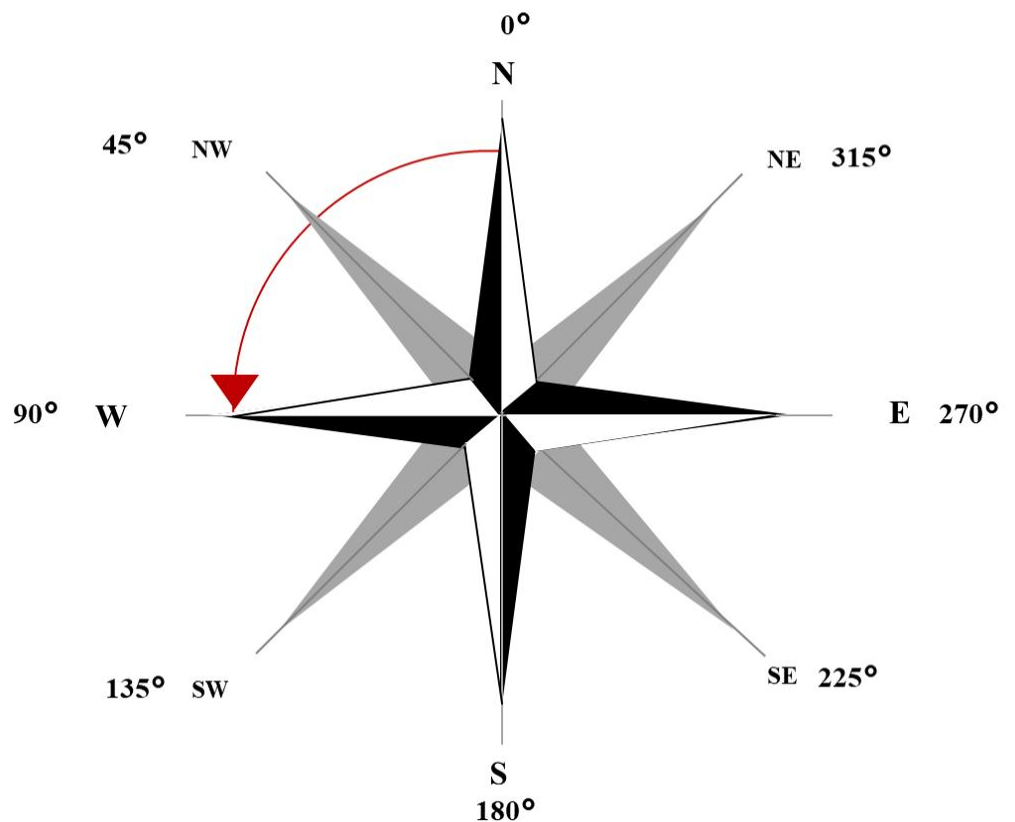


Figure 1. Main eight orientations of the urban environment used in the study.

In this study, we examine real buildings in their current orientation as well as hypothetical orientations. The orientations of 0° – 180° correspond to the extension of the urban canyon in the North-South and South-North directions, while 270° – 90° represent the extension in the East-West direction. Additionally, the orientations of 45° – 225° indicate the North West-South East extension, and 135° – 315° refer to the South West-North East extension. The specifications of each case study are summarized in Table 1.

Table 1. Features of the main building in case studies.

Sample	Height (m)	Floors	Length (m)	Total Area (m ²)
Case study 1/M1	50	17	291.3	2258.4
Case study 2/M2	45.4	14	208.5	2093.3
Case study 3/M3	37.3	9	202.8	2470.6

Figure 2 displays three selected residential buildings in Tallinn as case studies.

Table 2 outlines the characteristics considered when defining different scenarios during modeling and simulations for case studies 1 through 3.



Case study 1: XY coordination based on Google earth: $59^{\circ}24'51''N24^{\circ}44'18''E$
Harju county, Tallinn, Kesklinna district, Pärnu mnt 110



Case study 2: XY coordination based on Google earth: $59^{\circ}26'08''N24^{\circ}49'15''E$
Harju county, Tallinn, Lasnamäe district, Pae tn 68



Case study 3: XY coordination based on Google earth: $59^{\circ}25'57''N24^{\circ}46'45''E$
Address: Harju county, Tallinn, Kesklinna district, Vesivärava tn 50

Figure 2. Case studies, three residential buildings in Tallinn, Estonia.

The methodology of the study is designed in five steps, starting with step 0 to acquire data and finishing with step 4 to make an inventory and explain the application of the study.

According to Figure 3, the steps are in the following order:

- Step 0: Capturing data
- Step 1: Sampling
- Step 2: Simulation
- Step 3: Assessment
- Step 4: Application

Table 2. The general features of the simulated models.

Scenarios of Simulated Case Studies in the Different Extensions of the Canopy			
Model	Case Study	Orientation (°)	Extension
M1	Cs1	347	NE-SW
M2	Cs2	22	N-S
M3	Cs3	325	NE-SW
M1-1	Cs1	0	N-S
M1-2	Cs1	45	NW-SE
M1-3	Cs1	90	W-E
M1-4	Cs1	135	SW-NE
M1-5	Cs1	180	S-N
M1-6	Cs1	225	SE-NW
M1-7	Cs1	270	E-W
M1-8	Cs1	315	NE-SW
M2-1	Cs2	0	N-S
M2-2	Cs2	45	NW-SE
M2-3	Cs2	90	W-E
M2-4	Cs2	135	SW-NE
M2-5	Cs2	180	S-N
M2-6	Cs2	225	SE-NW
M2-7	Cs2	270	E-W
M2-8	Cs2	315	NE-SW
M3-1	Cs3	0	N-S
M3-2	Cs3	45	NW-SE
M3-3	Cs3	90	W-E
M3-4	Cs3	135	SW-NE
M3-5	Cs3	180	S-N
M3-6	Cs3	225	SE-NW
M3-7	Cs3	270	E-W
M3-8	Cs3	315	NE-SW

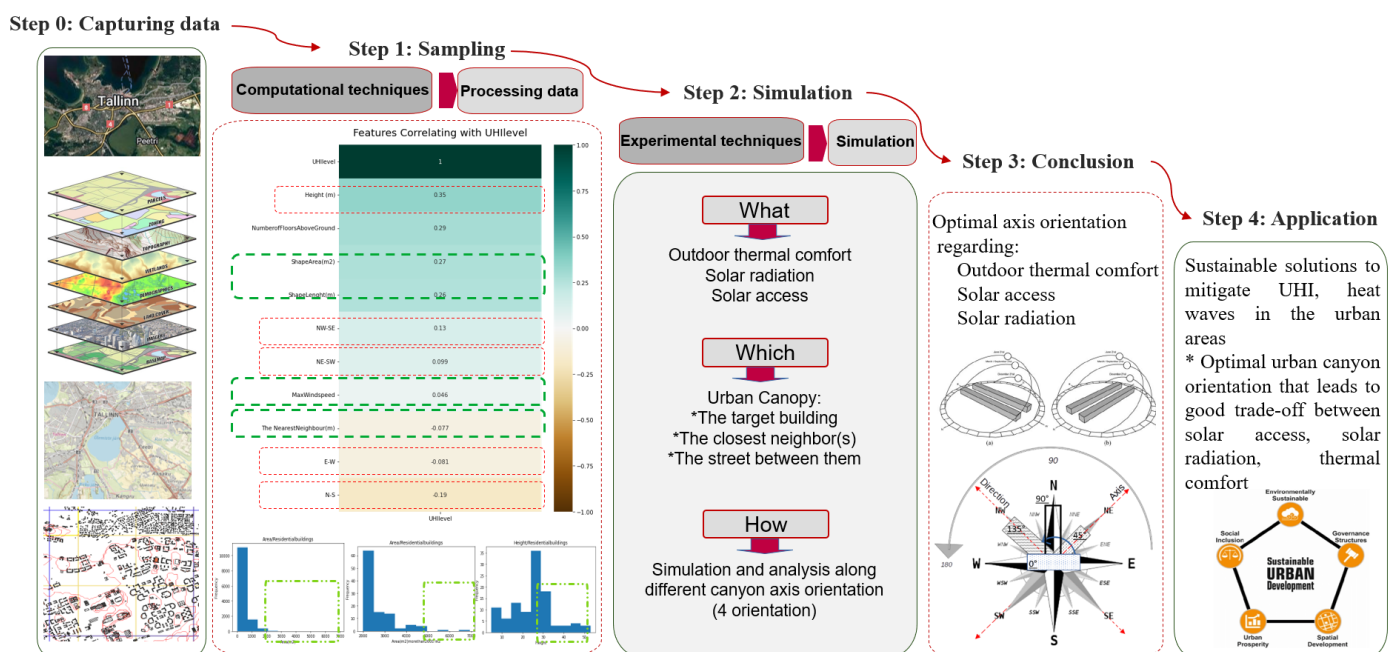


Figure 3. The framework for the study.

3.1. Step 0 “Urban Data Geoprocessing”

This research concentrates on the residential buildings with the greatest volume (maximum height and area) that went through an intense heatwave and UHI in 2014, 2018, and 2019. Moreover, case studies were chosen by sampling and utilizing the histogram to locate the more critical and more severe residential buildings from the Tallinn UHI dataset [34]. Thus, each case study is an actual building in Tallinn, Estonia (Lat. 59°26′ N Lon. 24°45′ E); the country has a humid continental climate with mild summers, as mentioned in the Köppen–Geiger classification in Dfb class [35] as Figure 4 shows.

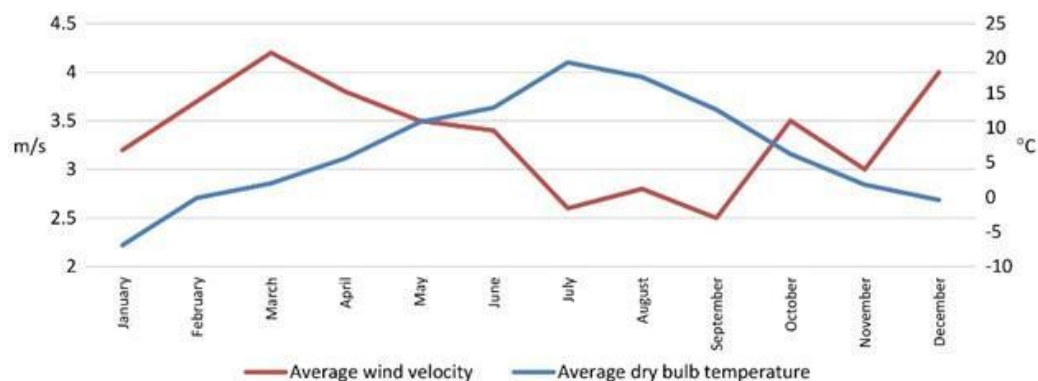


Figure 4. Monthly wind velocity and temperature averages of Tallinn, Estonia.

An extensive multidisciplinary presented dataset is collected with 34,001 building samples (rows) and 30 features (columns) in Tallinn, including the characteristics of the buildings, for example, Material, Height (m), Absolute Height (m), Number of Floors Above Ground, Shape Length (m), Shape Area (m²), the spatial indices of buildings on the hierarchical system grid, such as Built-up area (G200, level 1), Urban Density D1 (G200, level 1), Urban Density D2 (G1000, level 2), Urban Density D1 (G2000, level 3), Average Building Area in G200 (m²), Max Area in G200 (m²), Number of Buildings in G200, the defined indexes based on buildings and different zones in the city area, the Nearest Neighbour (m), Green Area in G200 (m²), the Ratio of Green Area/Grid Area (G200), Purpose of Building, Main Angle, Orientation, Height to Width (G200), the weather data on dates that the city experienced UHI phenomena, and the UHI value of each building [34,36].

The methodology to acquire data in the geoprocessed UHI dataset proposes a framework to categorize data into homogeneous or heterogeneous, static, or dynamic schemes and then collect data considering the homogeneous grid system [34]. Capturing data is the implementation of the hierarchical grid system in the data collection process:

- First, create a spatial index for each object and connect the objects to the grid system.
- Second, use the homogeneous ground to define urban indices mainly anchored in the heterogeneous data. The methodology uses the Python, Numpy, and Pandas libraries, the Geopandas package, and QGIS Tool. The approach helps to capture urban data from Tallinn GIS resources [37], taking into account the location, general characteristics, and other spatial properties of urban elements [34,37].

3.2. Step 1: Sampling, Finding Critical Urban Canyons

Our initial analysis investigated the relationship between the urban dataset and the Urban Heat Island (UHI) effect. The findings, depicted in Figure 5, revealed significant correlations and dependencies between various features of the dataset and UHI levels. Notably, we identified the size of the building, its height, and its area as influential factors affecting the UHI value. With this understanding, we focused our attention on the area and height of the buildings to identify large-volume structures in Tallinn using the collected data.

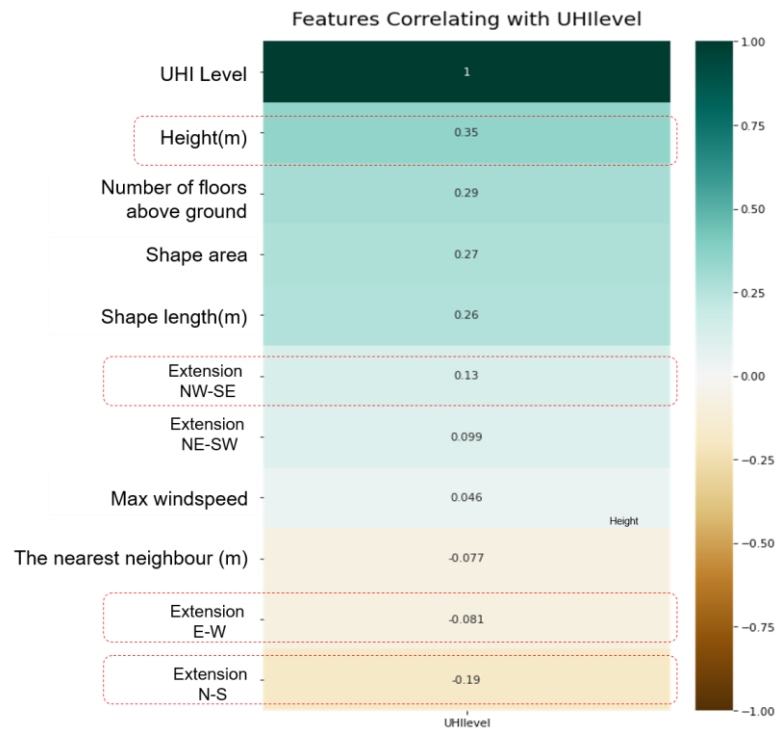


Figure 5. Dependency values between the features of the dataset and UHI level.

Moreover, our study placed particular emphasis on residential buildings, recognizing them as critical cases in the city, as they are susceptible to higher temperatures based on UHI data. To streamline our analysis, we initially filtered the dataset by prioritizing residential buildings, narrowing our focus.

As we delved into the analysis, we specifically examined the footprint area of the buildings. However, we discovered that the data exhibited a random distribution without any discernible patterns. Figure 6a visually represents this observation, indicating that buildings with a footprint area exceeding 2000 m² were less common in the dataset. Consequently, we conducted a more comprehensive investigation of the entire dataset, specifically targeting buildings with an area greater than 2000 m² to identify the infrequent occurrence of taller structures within this subset.

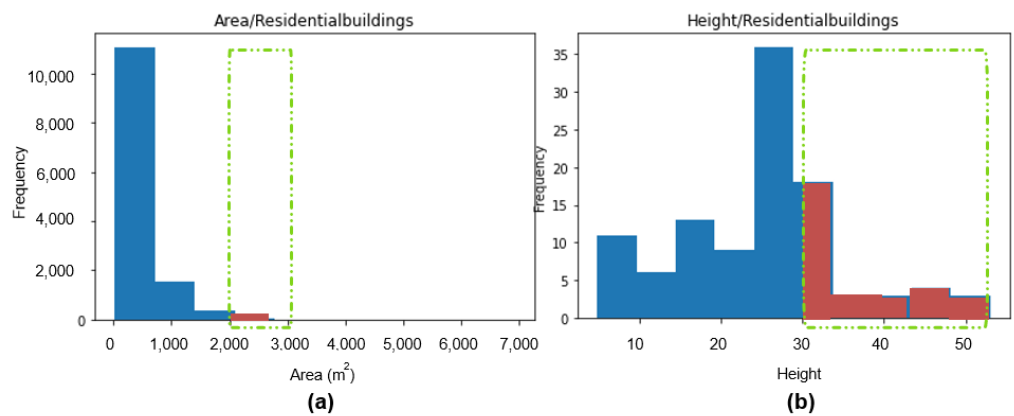


Figure 6. Sampling by using a histogram to choose case studies from the urban UHI dataset in Tallinn. (a) The highest value of the area in the residential buildings, (b) The highest value of the height in the residential buildings.

Thus, as the histogram shows, filtering the dataset to the highest volume buildings helps us to find which buildings are the critical cases to study. In addition, Figure 6a shows samples in the highest area and height of residential buildings in the UHI dataset (more correlated features with the UHI effect) with an area of more than 2000 m² and a height of over 30 m. Conversely, the graph shows fewer samples with an area higher than 2000 m² and a height higher than 30 m. Consequently, Figure 6b reveals samples that meet the research question's goal, pointing to some residential buildings in the UHI dataset with an area greater than 2000 m and a height above 30 m. The selected samples with an area of more than 2000 m and a height over 30 m are shown in red.

3.3. Step 2: Simulation in Building and Urban Scale

In step 2, we focused on the geometric modeling and simulation process of case studies in different scenarios (Table 2) to verify outdoor thermal comfort and solar access. Based on the sampling results and the UHI dataset, we have chosen three urban canyons with high-volume residential buildings in Tallinn, Estonia. The urban canopy layer refers to the space enclosed by the vertical boundaries of urban buildings, extending up to their rooftops [38].

To conduct CFD simulation, a three-dimensional computational model of fluid dynamics and energy balance, designed to simulate the microclimate of the study at the street level, was employed. The simulation uses ENVI-met, a software package specifically developed for urban microclimate modeling.

To evaluate outdoor thermal comfort, we employed the Physiological Equivalent Temperature (PET) index, which considers various factors that impact human thermal comfort, including air temperature, humidity, wind speed, and radiation. The PET index utilizes a range of thermal perceptions and physiological stress levels experienced by humans [39]. The PET index is based on the Munich Energy-balance Model for Individuals (MEMI). This two-node model simulates the thermal balance of the human body in a physiologically relevant way [40]. By utilizing this index, we were able to assess the thermal comfort of the outdoor environment across different scenarios and identify any potential issues related to heat stress and discomfort. The thermal perception and corresponding ranges of PET for each thermal comfort class are presented in Table 3. Additionally, we examined surface temperature, as it plays a crucial role in understanding the potential effects of absorbed solar radiation, which can contribute to increased surface temperatures, UHI effects [41], heat waves, and the overall thermal performance of buildings and outdoor spaces.

Table 3. The range of thermal index predicted thermal perception by human beings and physiological stress on human beings [39].

Thermal Perception Grade of Physiological Stress		
PET (°C)	Thermal Perception	Grade of Physiological Stress
4	Very cold	Extreme cold stress
8	Cold	Strong cold stress
13	Cool	Moderate Cold stress
18	Slightly cool	Slight cold stress
23	Comfortable	No thermal stress
29	Slightly warm	Slight heat stress
35	Warm	Moderate heat stress
41	Hot	Strong heat stress
	Very hot	Extreme heat stress

3.4. Step 3: Assessment and Results

Through the CFD simulation and analysis, output data related to the thermal comfort of people at the pedestrian level and the surface temperature of the urban area under different scenarios were acquired.

To evaluate thermal comfort, we used a comprehensive approach to evaluate the thermal performance of the studied urban area under different scenarios (Table 2). The first thermal comfort analysis is about finding the non-uniform spatial distribution of PET in each particular scenario in the urban canopy between the target building and the nearest neighbor.

The second analysis aims to create a model based on the scoring system to show uniform or normalized spatial distribution. The normalized PET of the urban canyon in each scenario is the weighted PET value by considering the quality and quantity of PET data. The highest value of the weighted PET leads us to find the optimal degree of orientation in the urban canyon.

The scoring system we implemented considers the thermal comfort level at each point in the canopy area. The scoring system allows us to calculate the overall level of comfortability at the pedestrian level by combining the scores of all the individual points. In addition, the surface temperature assessment of the studied areas was performed using the results of the CFD simulation. Overall, the orientations lead to the lowest surface temperature highlighted as the optimum building mass extension and taken into account in the final assessment to determine the best urban environment orientation to ensure comfortability.

3.5. Step 4: Application

Output data related to the optimal building mass orientation is helpful to suppose more sustainable solutions in cities. Furthermore, by improving outdoor thermal comfort and surface temperature in urban areas and leveraging UHI data, the study provides valuable insights into the thermal performance of the studied urban area.

The evaluation is particularly beneficial to guide urban planners and architects in proposing mitigation solutions to enhance thermal comfort in cities and create suitable conditions for achieving approved thermal comfort levels with complementary solar access in the city area. With this information, planners and architects can make more informed decisions about the design of new buildings, the placement of green spaces and other urban elements, and the use of shading devices and other technologies to reduce heat gain and improve outdoor thermal comfort.

Overall, the study's findings highlight the importance of considering outdoor thermal comfort and solar access in urban design and planning to create more livable and sustainable cities.

4. CFD Simulation and Numerical Analysis

The section is related to the CFD simulation and the numerical analysis to assess the outdoor thermal comfort and surface temperature in the studied areas. CFD simulation is used to simulate the microclimate of the studied area at the street level, considering the influence of various factors on thermal, such as air temperature, humidity, wind speed, and radiation.

By combining CFD simulation and numerical analysis, we can comprehensively understand the studied area's thermal performance under different scenarios. This information can then identify potential heat stress and discomfort issues and propose mitigation solutions to improve outdoor thermal comfort.

Table 4 and Figure 7 show more detailed information about the areas focused on CFD simulation and the area of the urban canyon in which PET results were evaluated.

Table 4. Detailed information about the CFD simulated areas of each case study.

Case Studies	Canopy Area (m ²)	Simulated Area (m ²)
Case study 1	20,650	5000
Case study 2	15,000	770
Case study 3	12,700	1400

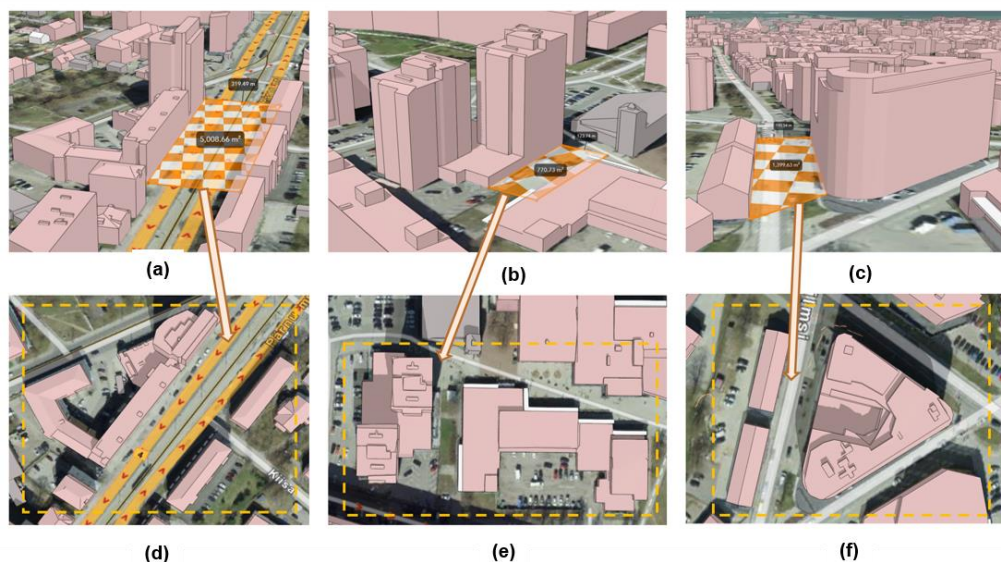


Figure 7. The canopy areas (the hatched rectangular shapes) and the whole simulated areas of each case study (the dashed rectangular shapes). (a) The canopy area, cases study 1, (b) The canopy area, cases study 2, (c) The canopy area, cases study 3, (d) The whole simulated area, case study 1, (e) The whole simulated area, case study 2, (f) The whole simulated area, case study 3.

Different scenarios of case studies were simulated based on the specific orientation of the canopy extension, including east-west (E-W), north-south (N-S), southeast-northwest (SE-NW), and northeast-southwest (NE-SW), as shown in Table 2. Additionally, Table 4 provides details on the simulation area and the corresponding canopy coverage area for each model. Moreover, the canopy area and simulated area for each scenario were determined based on the information presented in Table 4. The geometry modeling process took into account the real physical attributes of the case studies described in Table 1.

In order to perform the CFD simulation using ENVI-met, specific inputs are required, including information about the surrounding environmental features and meteorological data. Additionally, the construction system of the buildings and the surface materials within the simulated urban areas are defined using the material library provided by ENVI-met. For instance, the envelope of the models was defined using a concrete material with moderate insolation properties, which was available in the ENVI-met software's database. Moreover, precise calculations of solar reflectivity and radiation values were conducted, taking into account the specific date, time, and location of the case studies, in order to determine the sun's position during the simulation.

4.1. Meteorological Setting

The input data for the simulation models are the physical properties of the studied urban areas (buildings, soil, and vegetation) and geographic and meteorological data [30].

This study conducted the CFD simulation on 25 July 2014, during a high UHI and heat wave period [37]. The simulated period lasted from 16:00 to 17:00, including the maximum air temperatures during a summer day of 28 °C. The outdoor thermal comfort assessment was conducted at 17:00 and evaluated at 1.80 m, the average human height.

Simple forcing was used in all scenarios to adjust for the meteorological conditions, creating a 24-h weather data cycle that defined the meteorological boundary conditions for the ENVI-met simulation.

Table 5 gives information about the weather condition of Tallinn on the supposed date and time that was chosen for the CFD simulation.

Table 5. The input meteorological data during the CFD simulation by ENVI-met.

Date, 25 July 2014. Time: 17:00	
Air temperature (°C)	Max 28/Min 17
Max relative humidity (%)	Max 75/Min 45
Wind speed at inflow border (m/s)	2.00
Wind direction at inflow (°)	90.00
Roughness length (m)	0.010
Specific humidity in 2500 m (g/kg)	8.00

4.2. Outdoor Thermal Comfort Assessment, PET

PET, expressed in °C, is based on the human energy balance model MEMI and includes the physiological thermoregulatory processes of human beings to adjust to a climatic situation outdoors. The thermal comfort zone for the PET index was initially defined as 18–20 °C [30]. The other classes of thermal comfort are mentioned in Table 3.

In this section, the authors listed all the parameters used in the CFD simulation. In addition, during the simulation, the building's indoor temperature was set to a constant value of 20 °C. Therefore, the outside microclimate did not influence the building temperature. Overall, using the PET index and CFD simulations is a useful approach to assess the thermal comfort of the studied area. Furthermore, by taking into account the physiological thermoregulatory processes of human beings and using advanced simulation techniques, a more accurate and comprehensive understanding of outdoor thermal comfort in urban areas will achieve.

Personal Parameters

Thermal comfort is a subjective concept that depends on personal features and describes a person's state of mind regarding whether they feel comfortable [42]. Thus, once the meteorological data and environmental characteristics are added to the input data used in the CFD simulation, thermal comfort in PET indices needs to set the individual personal data that are supposed as the users of the urban areas. In this study, PET is taken as the outdoor thermal comfort assessment and calculated just for a male pedestrian wearing very light summer clothes standing with a walking speed of 1.2 m/s. For a simple PET assessment process, just male pedestrians wearing unique clothing values with normal body parameters were considered. Table 6 shows other personal parameters used in PET evaluation.

Table 6. Personal parameters applied in PET assessment in ENVI-met simulations.

Basic Personal Parameters	
Age of the person	35
Weight (kg)	75
Height (kg)	1.75
Surface area of the body (sm ²)	1.91
Clo	0.10
Metabolic work (W)	164.70

5. Results

5.1. Surface Temperature

The assessment of the surface temperature of the urban canopy in each scenario is a valuable approach to understanding the impact of changes in canopy orientation on the urban temperature. By analyzing the minimum, maximum, and median values of surface temperature, we can identify the optimum orientation of the canopy for maximizing thermal comfort and decreasing temperatures of urban surfaces. Furthermore, surface temperature is a critical measure in assessing the UHI effect, as it indicates the level of heat absorbed by the surfaces of the urban environment. Thus, by reducing surface temperature, it is possible to mitigate the UHI effect and improve thermal comfort for pedestrians.

Through the surface temperature analysis, we can determine the impact of canopy orientation on surface temperature and identify the optimal orientation that reduces surface temperature and maximizes thermal comfort. This information can inform urban planning and design strategies prioritizing thermal comfort and sustainability. It is important to consider these orientations as they can cause more heat on urban surfaces and potentially result in lower thermal comfort levels for pedestrians.

According to Figure 8a,b, in case studies 1 and 2, scenarios M1-8, M1-6 (24.9 and 28.3 °C) and M2.8, M2.6 (24.3 and 24.4 °C) have the lowest median surface temperatures when oriented at 315° and 225°, respectively. This suggests that these orientations can provide the highest thermal comfort for pedestrians in the case studies. Likewise, Figure 8c shows in case study 3, the median surface temperature data is observed in M3-5 and M3-4 (22.4 and 23.6 °C) with orientations of 180° and 135°, respectively. The finding indicates that these orientations can also provide high thermal comfort for pedestrians in this case study. Furthermore, in case study 1, the orientations with the highest median of surface temperature are M1-1, M1-2, and M1-3 with orientations of 0°, 45°, and 90°, respectively. In case study 2, the orientations with the highest median of surface temperature are M2-1, M2-4, M2-2, and M2-3 with orientations of 0°, 135°, 45°, and 90°, respectively. Finally, in case study 3, the orientations that cause the highest median of surface temperature in the analyzed areas are M3-2, M3-1, M3-3, and M3-8 with orientations of 45°, 0°, 90°, and 315°, respectively.

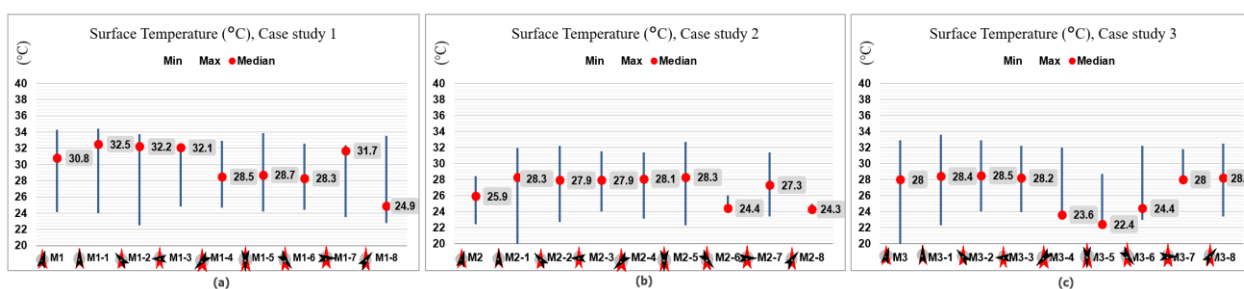


Figure 8. Results of surface temperature (°C) in the urban canopy of different scenarios. (a) Case study 1, (b) Case study 2, (c) Case study 3.

This section presents the results of outdoor thermal comfort, expressed in terms of the PET index and surface temperature in degree centigrade (°C), to choose the best orientations in each case study to lead to the highest comfort level. The spatial distribution of outdoor thermal comfort in terms of the metric PET was calculated via simulation for 27 scenarios of three case studies. The thermal comfort assessment results are explained in two forms, non-uniform and normalized spatial distribution of PET.

5.2. Non-Uniform Spatial Distribution of PET

Figures 9–11 show the initial results of PET assessed for case studies in a different scenario considering the input setting, meteorological data, and parameters during the CFD simulation in the defined canyon orientation, according to Table 2.

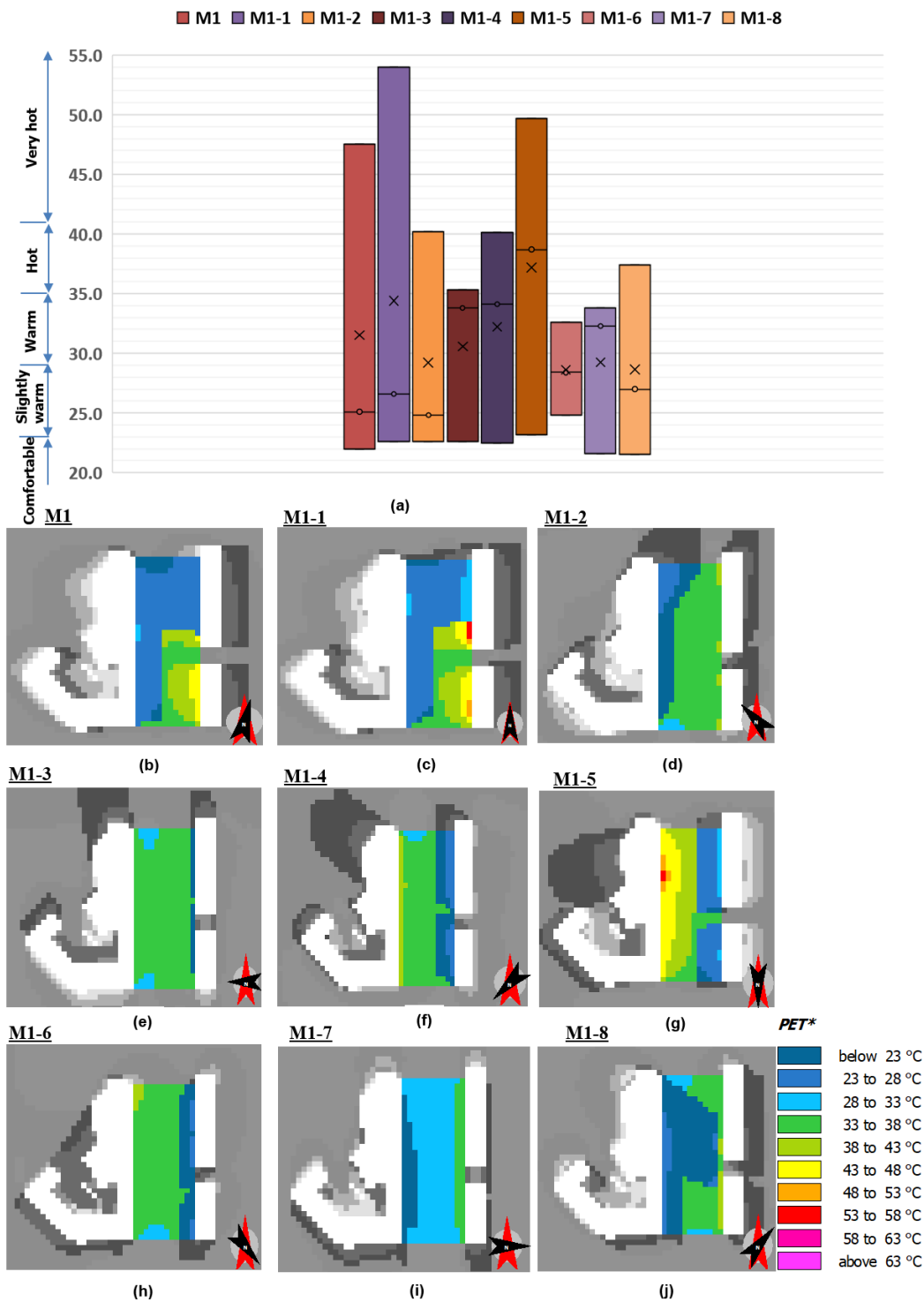


Figure 9. Graphical distribution of PET in different canyon orientations, obtained from CFD simulation, cases study 1, Scenarios: M1, M1-1 to M1-8. The minimum, maximum, and average scores stand out prominently within the box plots, resembling a star. For the configuration shown in (a) The box plot shows the minimum, average, median, and maximum of PET in each scenario, spatial distribution of PET, (b) M1 (c) M1-1, (d) M1-2, (e) M1-3, (f) M1-4, (g) M1-5, (h) M1-6, (i) M1-7, (j) M1-8.

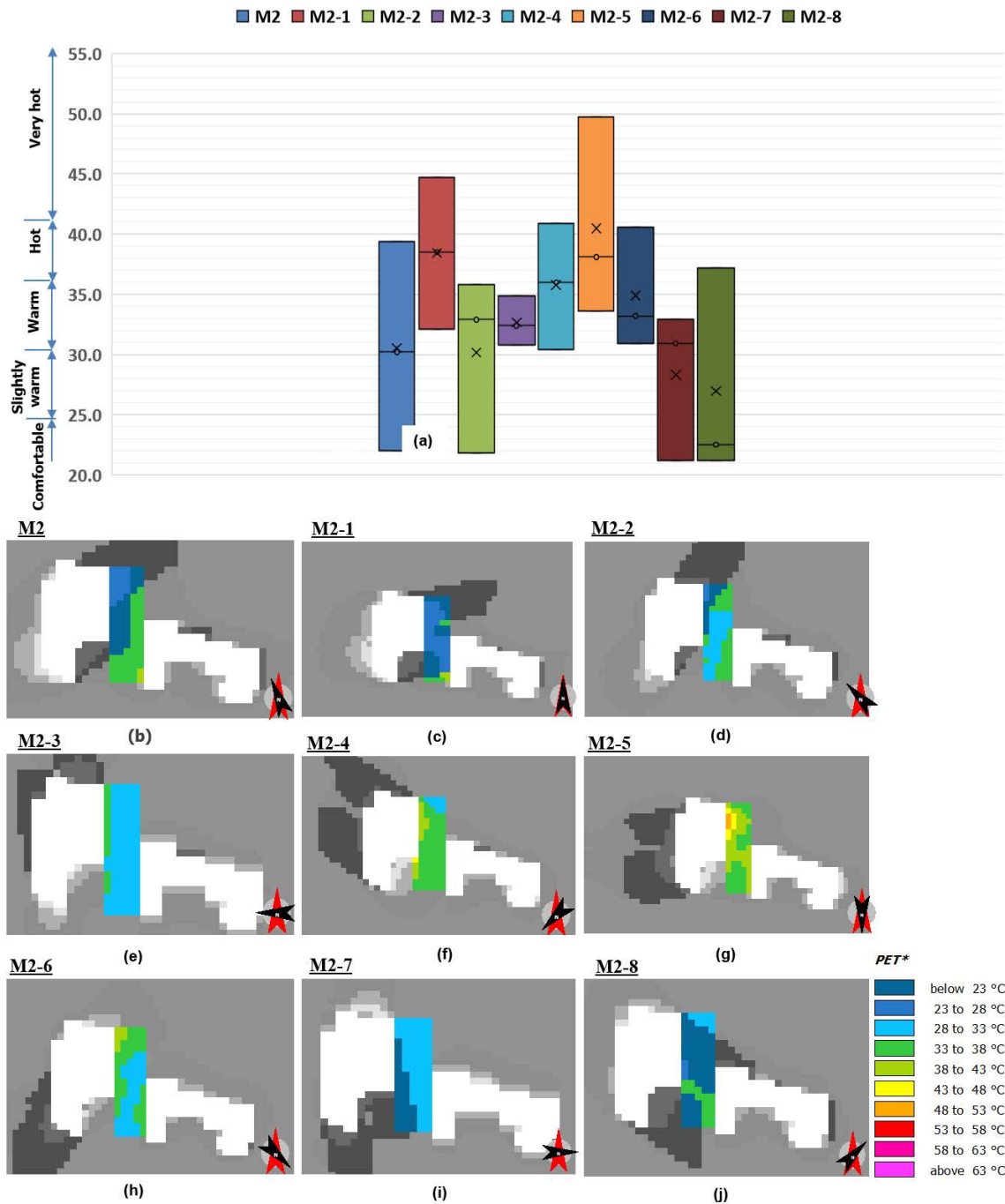


Figure 10. Graphical distribution of PET in different canyon orientations, obtained from CFD simulation, cases study 2, Scenarios: M2, M2-1 to M2-8. The minimum, maximum, and average scores stand out prominently within the box plots, resembling a star. For the configuration shown in (a) The box plot shows the minimum, average, median, and maximum of PET in each scenario, Spatial distribution of PET, (b) M2 (c) M2-1, (d) M2-2, (e) M2-3, (f) M2-4, (g) M2-5, (h) M2-6, (i) M2-7, (j) M2-8.

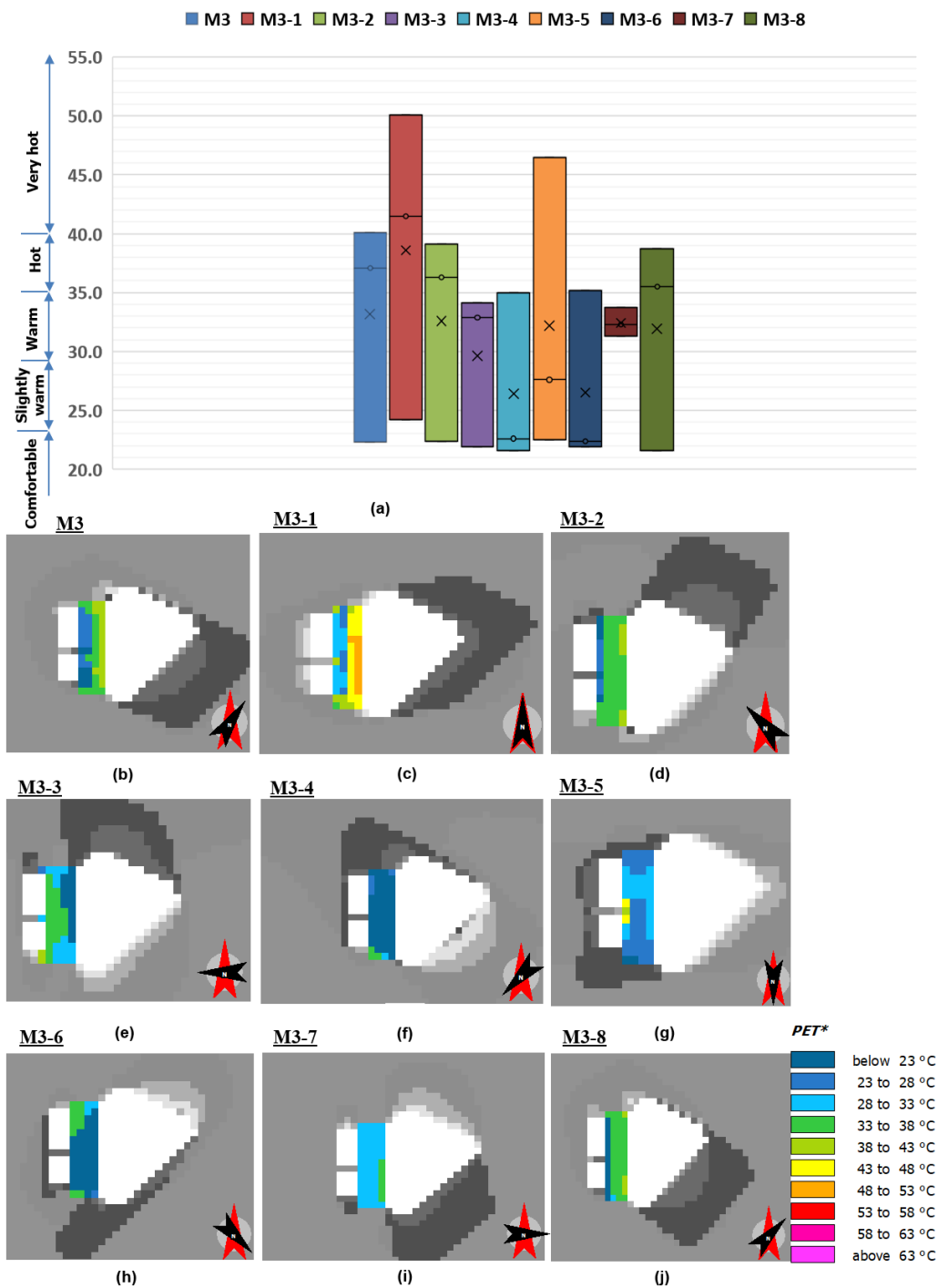


Figure 11. Graphical distribution of PET in different canyon orientations, obtained from CFD simulation, cases study 3, Scenarios: M3, M3-1 to M3-8. The minimum, maximum, and average scores stand out prominently within the box plots, resembling a star. For the configuration shown in (a) The box plot shows the minimum, average, median, and maximum of PET in each scenario, spatial distribution of PET, (b) M3, (c) M3-1, (d) M3-2, (e) M3-3, (f) M3-4, (g) M3-5, (h) M3-6, (i) M3-7, (j) M3-8.

For example, in Figure 9, the initial results of PET assessment in different scenarios of case study 1 are demonstrated. Furthermore, Figures 10 and 11 show the results of the PET assessment of case studies 2 and 3, respectively.

It can be seen in the box plot in Figure 9. However, the minimum value of PET of all scenarios is almost the same; scenarios have different values in the average, median, and maximum of PET. Likewise, M1, with the original orientation of 347° (North East-South West), has the lowest minimum value of PET while the other values are even higher than others. Moreover, M1-1 and M1-5, with the orientation of 0 and 180°, have the highest value of the maximum and median of PET. Likewise, a comparison of all different orientations in the urban canopy of case study 1 indicates M1-2 with the orientation of 45° has the lowest median of PET value rather than other scenarios.

In conclusion, the non-uniform spatial distribution of PET does not give us comprehensive data to interpret the results and understand two meanings: (1) in which scenario does the urban canyon offer a better level of thermal comfort in PET at the pedestrian level? (2) in which scenario most of the area is in the comfort zones of PET, such as comfortable (18–23 °C) and slightly warm (23–35 °C).

Thus, there are different measures of PET, such as the minimum, maximum, median, and average values, which can vary depending on the scenario. However, based on the initial evaluation of PET of the simulated scenarios, it is impossible to conclude which orientation offers a higher level of thermal comfort. Therefore, PET's non-uniform spatial distribution can make it challenging to interpret the study results and draw definitive conclusions about which scenario offers a better level of thermal comfort in PET at the pedestrian level.

5.3. Normalized Spatial Distribution of PET

According to Joshi et al., measuring subjective experiences or phenomena can be challenging, as they are often difficult to quantify using conventional measurement techniques [35]. Thus, to obtain the most comprehensive analysis and find the optimum orientation of the urban canopy in the scenarios, we need to consider both the frequency of PET data in each level and the maximum and minimum PET, as well as the average in each urban canyon.

Therefore, evaluation scales can be presented in various graphical ways, with different levels of detail, and no standard gives specifications on the choice of the most suitable configuration; thus, the selection is often a matter of the specifications of the study [43].

In the study, Nazarian et al. used the continuous Outdoor Thermal Comfort Autonomy (OTCA) scale as a metric to measure outdoor thermal comfort. According to the authors, OTCA considers the percentage of time an outdoor space is within the desired thermal comfort range, including periods where the thermal comfort level is below the threshold. It is an extension of Spatial OTCA, defined as the percentage of outdoor space within the desired thermal comfort range at least half of the occupied time (over a year or a prescribed period of use) [44].

Here, we designed a weighted scale to consider the level of thermal comfort in studied areas and rank the data of PET based on the frequency of data in each PET class. As a widespread scale used in different areas such as psychology, sociology, health care, marketing, attitude, preference, customers' quality perceptions or expectations, and subjective well-being in health care, Likert scales have wide applications in different science [45]. In addition, Likert scales are examples of such scales in psychometrics used widely in social science & educational research [46]. Therefore, we applied the Likert scale to weigh the PET classes and ranked the importance of data in each thermal comfort level.

Figure 12 shows the Likert scaling system applied in the study.

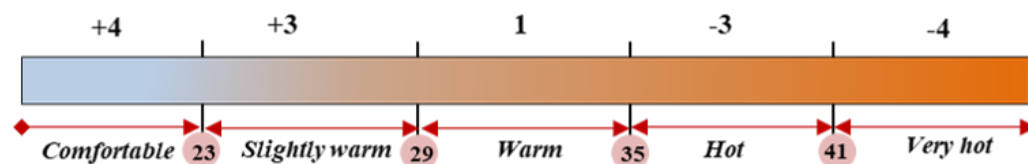


Figure 12. Five-point Likert scale was used in the PET analysis of scenarios.

Each item in the Likert scale usually has an odd number of response categories, to five or seven levels [45], and is named the five-point or seven-point Likert scale. Here, we applied five points Likert scale by considering the comfortability of the area that the Likert scale should measure and assigning the highest indicator equals +4 to the PET class of Comfortable, +3 to Slightly warm, +1 to Warm, and the negative scores to the worst classes of PET cause a high level of discomfort in the urban area, meaning −3 and −4 to Hot and Very hot classes.

Statistical Methods and Exploration of Data

In this section, to better interpret the results, calculating the overall thermal comfort level of each scenario, not only considering the arithmetic and mathematical average of PET but also taking into account the frequency of data in each level of PET, is essential. Therefore, it is an excellent approach to consider the frequency of data in each level of PET to better interpret the results of each scenario’s overall thermal comfort level. Accordingly, at first, we stored the results of the PET assessment of each scenario as the experimental data in a matrix and split them into five levels of thermal perception.

To describe a process of analyzing the results of a study on thermal comfort levels in different urban scenarios, we should mention that, at first, the results of the PET assessment of each scenario as the experimental data in were split into five levels of thermal perception based on five-point Likert scale. To better understand the distribution of PET data in each thermal comfort level, we created an experimental matrix and pie charts that show the percentage of PET data distribution of scenarios in different classes of PET, Figures 13–15.

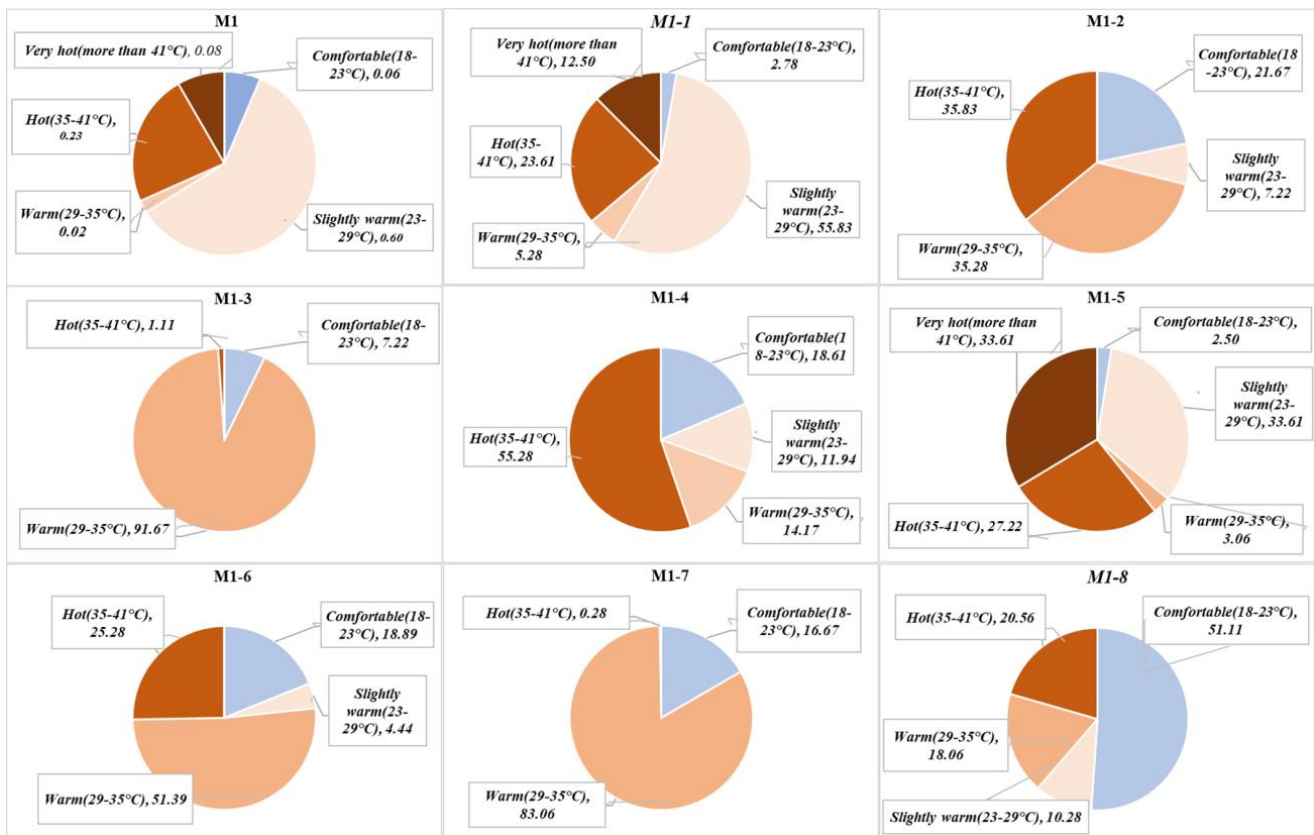


Figure 13. The distribution of PET data in each class of PET/Case study 1 (The total of all segments in every pie chart amount to 100%).



Figure 14. The distribution of PET data in each class of PET/Case study 2 (The total of all segments in every pie chart amount to 100%).

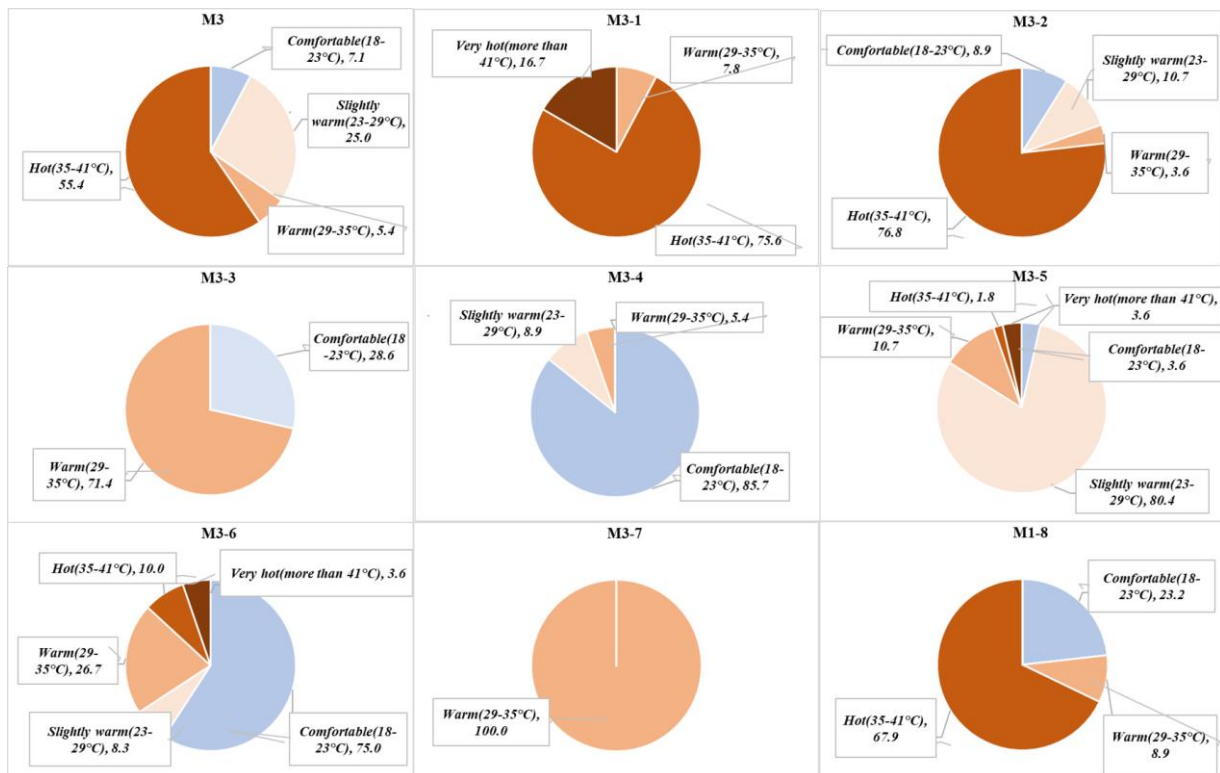


Figure 15. The distribution of PET data in each class of PET/Case study 3 (The total of all segments in every pie chart amount to 100%).

The experimental matrix contains the thermal perception of all scenarios and PET’s arithmetic average (mathematical average) in each thermal comfort level, starting from comfortable to very hot. Moreover, the quantity of PET data in each thermal comfort level is counted to understand how much each urban area in the urban canopy offers the considered thermal comfort level. To further refine the analysis, we applied the Likert scaling system to assign a score to each thermal comfort level, which reflects its importance. Combining the arithmetic average of PET in each thermal comfort level with the weight or value of each thermal perception level and the quantity of PET data in each level makes it possible to obtain a more accurate and meaningful measure of each scenario’s overall thermal comfort level.

Thus, we defined a statistical method that uses the arithmetic average of PET in each thermal comfort level, starting from comfortable, PET lower than 23° as the comfort zone to greater than 41° to as the zone with the very hot comfort level.

The next step is calculating the statistical average of each PET level by multiplying the arithmetic average of each PET level by the weights of the Likert scale and the respective count of data in each PET level. The following formula shows the weighted mean of PET used in the PET exploration method.

$$\text{Weighted Mean (Wm)} = \frac{\sum_{ni=1}^n (xi * wi)}{\sum_{ni=1}^n wi}$$

$$Wm = w_1x_1 + w_2x_2 + \dots + w_nx_n / w_1 + w_2 + \dots + w_n$$

where: \sum denotes the sum

w is the weights, and x is the value of PET

In cases where the sum of weights is 1,

$$Wm = \sum_{ni=1}^n (xi * wi)$$

Figure 16 is the schematic diagram of the model to evaluate PET in each scenario.

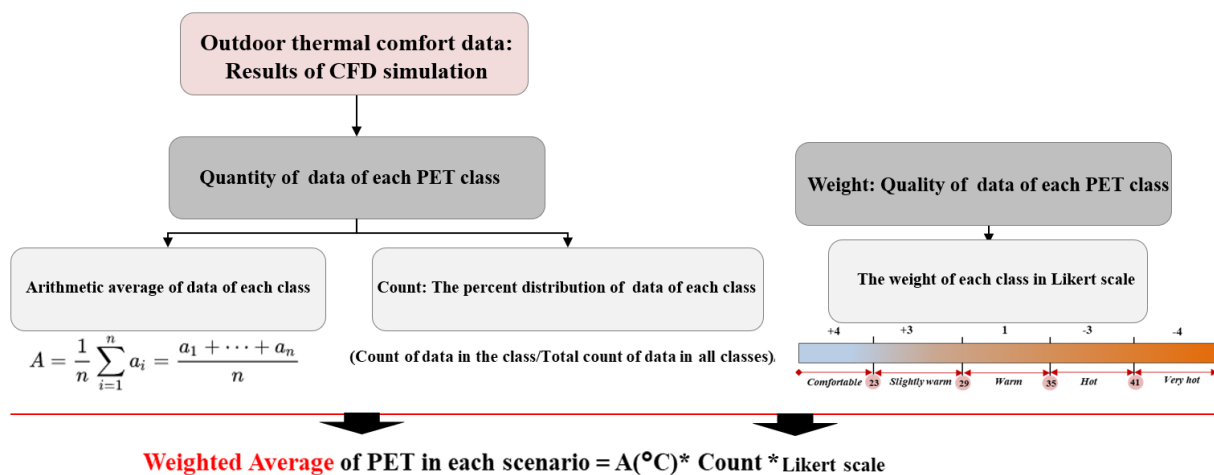


Figure 16. The evaluation model of PET value.

5.4. Analyzing Data Based on the Evaluation Method

The next step was calculating the statistical average of each PET level. For example, to calculate the weighted mean of PET (Wm-PET) for scenario M1, we multiplied the arithmetic average of each PET level (22.5, 24.6, 34.5, 38, and 43.4) by the weights of each response in the Likert scale (4, 3, 1, −3, and −4), and then multiplied each of those values by the count of responses (0.064, 0.597, 0.022, 0.233, and 0.083).

For example, for PET level 1 (Comfortable), the weighted score (W_s) would be:

$$(22.5 * 4 * 0.064) = 5.76$$

We repeated this process for each PET level and then summed up the weighted scores for all PET levels to obtain the overall weighted mean for PET in scenario M1. The calculation for the overall weighted mean is:

$$\begin{aligned} Wm_PET, M1 &= (W_s_PET_level1) + (W_s_PET_level2) + \dots + (W_s_PET_level5) \\ &= (22.5 * 4 * 0.064) + (24.6 * 3 * 0.597) + (34.5 * 1 * 0.022) + (38 * (-3) * 0.233) + (43.4 * (-4) * 0.083) \\ &= 5.7 + 44.1 + 0.8 - 26.6 - 14.5 = 9.5 \end{aligned}$$

Therefore, the weighted mean of PET in scenario M1 is 9.5, which represents the overall level of perceived exertion for this scenario, taking into account both the quantity of data in PET classes and the weight of each class as well as the arithmetic average of data of PET in each level. To report the result regarding the optimal orientation for achieving the highest thermal comfort in different scenarios, the summarized weighted average of each scenario is shown in Figure 17.

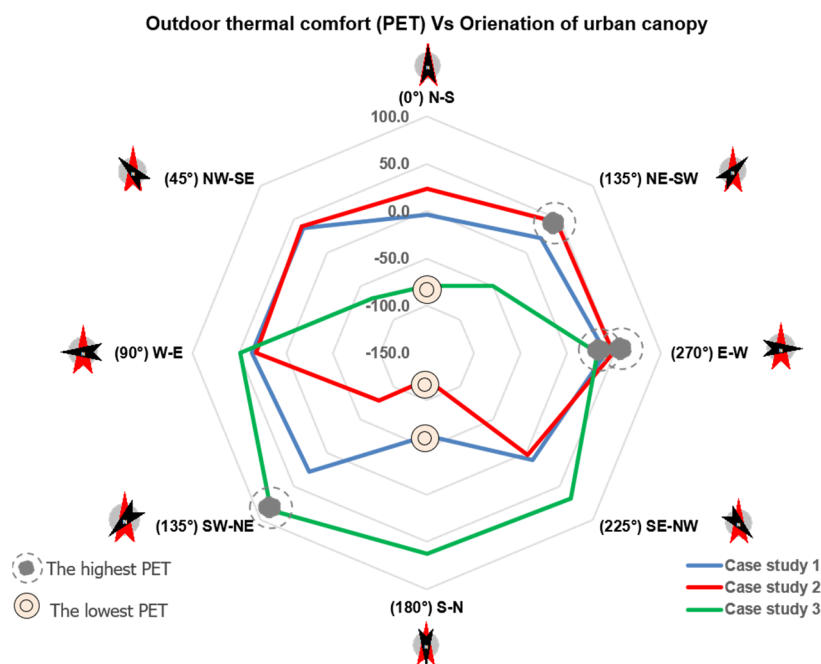


Figure 17. The results of weighted average of PET of each case study in different orientations of the urban canopy.

According to the data presented in Figure 17, the PET index indicates that the highest level of thermal comfort in case study 1 is observed when the urban canyon is oriented in the East-West direction (270°) in scenario M1-7. In case studies 2 and 3, the highest PET levels are seen in scenarios M2-7 and M3-4, respectively, with orientations of 270° (East-West) and 135° (South West-North East) for the extension of the urban canyons. The assessment of outdoor thermal comfort in the studied case studies reveals that the canopy extension in the North-South direction yields the lowest thermal comfort value in all three cases. This is attributed to the sun's high angle during the day, which can create hot and uncomfortable conditions in these orientations. It is important to note that the optimal orientation for achieving outdoor thermal comfort varies depending on the specific characteristics of each case study, as Figure 17 shows.

6. Discussion

Figure 18 presents the study’s findings, indicating that the West-East and East-West orientations offer the best outdoor thermal comfort and lowest surface temperatures across all examined case studies and simulation scenarios. However, it is crucial to consider the location of the tallest wall within the urban canyon, as this significantly affects thermal comfort and surface temperatures. Furthermore, the study reveals that the North East-South West orientation provides optimal thermal comfort for case studies 1 and 2 at the pedestrian level. Still, it yields lower thermal comfort for case study 3. Conversely, the South West-North East orientation offers optimum outdoor thermal comfort for case studies 1 and 3. In contrast, the South East-North West orientation only provides good thermal comfort for case study 3. Consequently, the optimal orientation of canopies varies depending on the specific characteristics of each case study, the surrounding environment, and the level of sun exposure and shading on the surfaces. When a tall building is present on one side of a canyon or street, the orientation of the canopy becomes crucial in determining the thermal comfort levels in shaded areas. For instance, in case studies 1 and 2, extending the canopy from North East to South West does not offer sufficient shading due to the orientation of the taller building on the left side of the canyon, potentially resulting in discomfort at the pedestrian level. In contrast, in case study 3, where the taller wall of the canopy is located on the right side, extending the canopy from South West to North East provides better shading and enhances thermal comfort. Therefore, it is vital to consider the specific morphological features of buildings and the surrounding area when designing urban canopies.

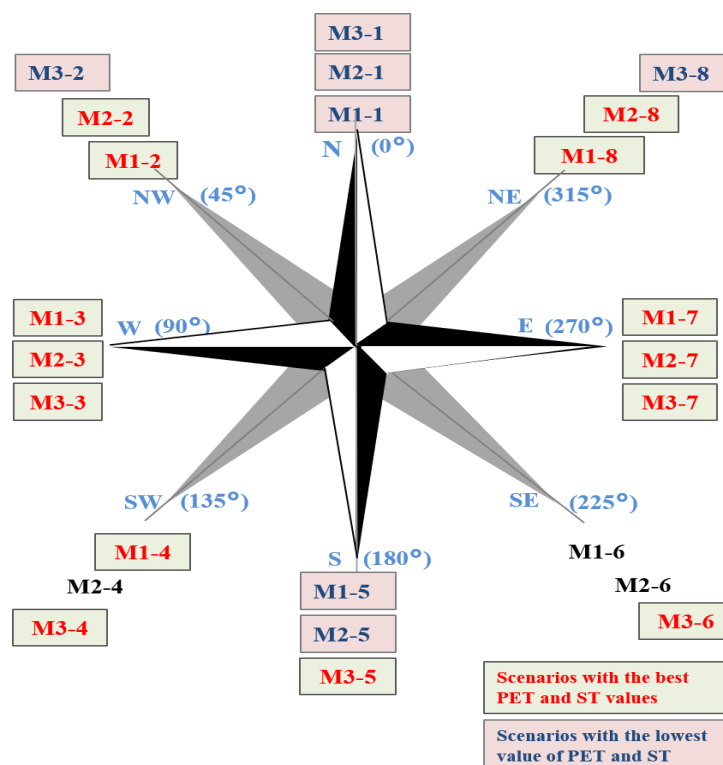


Figure 18. Final results regarding optimum thermal comfort and surface temperature of each scenario in different urban environment orientations.

Step 4: Application of the Study

The study underscores the significant influence of urban canyon orientation on thermal comfort and surface temperature within urban settings. By considering the orientation of urban canopies, urban planners and designers can optimize urban environment design to prioritize the well-being of residents and visitors. The findings offer insights into de-

termining the optimal extension of the canopy layer to maximize thermal comfort, thus providing more comfortable areas for pedestrians. Overall, these findings are valuable for urban planners and designers seeking to develop more sustainable and livable urban environments that prioritize the well-being of individuals. Moreover, considering the specific characteristics of the urban canyon enables planners to implement targeted strategies, including shading, ventilation, and other measures, to enhance outdoor thermal comfort and mitigate the effects of phenomena including the UHI effect.

7. Conclusions

This investigation focused on the impact of urban canopy orientation on outdoor thermal comfort and surface temperature in areas with significant UHI effects. Numerical analysis and CFD simulations were employed to evaluate these factors in urban environments. The orientation of urban environments, buildings, and streets within urban canyons is crucial in determining thermal comfort levels. The level of thermal comfort and surface temperature is influenced by factors such as building mass, canopy wall height, and arrangement. The study's findings underscore the significance of the canopy orientation in determining thermal comfort levels in shaded areas when there is a tall building present on one side of a canyon or street. The research highlights that the optimal orientation of canopies depends on the unique characteristics of each case study, the surrounding environment, and the degree of sun exposure and shading on surfaces. It emphasizes the importance of considering the buildings and elements surrounding them when designing and positioning canopies to achieve optimal thermal comfort in shaded areas affected by tall buildings. By incorporating these factors into the design and planning processes, urban planners and designers can create comfortable and sustainable living spaces. The assessment of outdoor thermal comfort within the urban canopy provides valuable insights for optimizing the extension of the canopy layer, enhancing thermal comfort, controlling the UHI effect, and improving residents' quality of life. The findings have broad applicability and can assist in early-stage city design, redevelopment, and renovation projects. Prioritizing outdoor thermal comfort in urban design offers social, environmental, and economic advantages.

While the study's findings are specific to Tallinn, the methodology and approach we employed for assessing thermal comfort and surface temperatures have broader applicability and can be implemented in various locations and climates. This can be achieved by considering the unique characteristics of the built environment and meteorological conditions of each area. However, further research is needed to formulate effective policies and planning codes that can adequately tackle the variations in Urban Heat Islands, manage excessively hot urban regions, and enhance thermal comfort. It is essential to base mitigation strategies for UHI on the specific thermal attributes of the particular urban area rather than relying solely on distinctions between urban and rural zones. Moreover, when adapting thermal comfort indices to diverse climates and countries, cultural differences should also be taken into consideration.

Limitations of the Study

It is crucial to acknowledge and consider the limitations of any study to ensure that the results are not overgeneralized. In this study, several limitations should be taken into account. To begin with, the geometric models used for the CFD simulations were simplified by omitting detailed information regarding the systems, materials, and albedo of the models. This simplification has the potential to impact the accuracy of the obtained results. The thermal comfort assessment in the study was also limited to a specific subset of the population, namely males in light clothing and seated position. This limitation calls for future studies to include a more diverse population, especially vulnerable groups such as the elderly and children, and gather data on their physical characteristics, clothing choices, and activity levels to provide a more comprehensive analysis of the impact of thermal comfort on different individuals.

Furthermore, it is important to note that thermal comfort is just one aspect related to the UHI effect in urban areas. Future studies should aim to provide a more holistic understanding of UHI by considering other strategies and elements of the urban environment and their configurations. Lastly, it should be acknowledged that the optimal orientation for achieving thermal comfort in an urban canyon can vary depending on various factors, such as the local climate, building materials used, and the layout of the urban canyon itself. Considering all these factors will contribute to more accurate and reliable results.

Author Contributions: Conceptualization, N.E., A.S., F.D.L. and S.B.Y.; Methodology, N.E., A.S., F.D.L. and S.B.Y.; Software, N.E.; Formal analysis, N.E., F.D.L. and S.B.Y.; Data curation, N.E.; Writing—original draft, N.E.; Writing—review & editing, N.E., A.S., F.D.L., K.S.L. and S.B.Y.; Visualization, N.E.; Supervision, A.S., F.D.L., K.S.L. and S.B.Y. All authors have read and agreed to the published version of the manuscript.

Funding: The European Commission has supported this work through the H2020 project Finest Twins (grant No. 856602).

Data Availability Statement: <https://data.mendeley.com/datasets/xm92bw2f49/1>.

Conflicts of Interest: The authors declare no conflict of interest.

References

1. Akbari, H.; Cartalis, C.; Kolokotsa, D.; Muscio, A.; Pisello, A.L.; Rossi, F.; Santamouris, M.; Synnefa, A.; Wong, N.H.; Zinzi, M. Local climate change and urban heat island mitigation techniques—The state of the art. *J. Civ. Eng. Manag.* **2016**, *22*, 1–16. [[CrossRef](#)]
2. Erell, E.; Pearlmutter, D.; Williamson, T. *Urban Microclimate: Designing the Spaces between Buildings*; Urban Microclimate; Routledge: London, UK, 2012. [[CrossRef](#)]
3. Onishi, A.; Cao, X.; Ito, T.; Shi, F.; Imura, H. Evaluating the potential for urban heat-island mitigation by greening parking lots. *Urban For. Urban Green.* **2010**, *9*, 323–332. [[CrossRef](#)]
4. Aflaki, A.; Mirnezhad, M.; Ghaffarianhoseini, A.; Ghaffarianhoseini, A.; Omrany, H.; Wang, Z.-H.; Akbari, H. Urban heat island mitigation strategies: A state-of-the-art review on Kuala Lumpur, Singapore and Hong Kong. *Cities* **2017**, *62*, 131–145. [[CrossRef](#)]
5. Mirzaei, P.A.; Haghighat, F. Approaches to study urban heat island—abilities and limitations. *Build. Environ.* **2010**, *45*, 2192–2201. [[CrossRef](#)]
6. Sagris, V.; Sepp, M. Landsat-8 tirs data for assessing urban heat island effect and its impact on human health. *IEEE Geosci. Remote Sens. Lett.* **2017**, *14*, 2385–2389. [[CrossRef](#)]
7. Aleksandrowicz, O.; Vuckovic, M.; Kiesel, K.; Mahdavi, A. Current trends in urban heat island mitigation research: Observations based on a comprehensive research repository. *Urban Clim.* **2017**, *21*, 1–26. [[CrossRef](#)]
8. Vásquez-Álvarez, P.E.; Flores-Vázquez, C.; Cobos-Torres, J.-C.; Cobos-Mora, S.L. Urban Heat Island Mitigation through Planned Simulation. *Sustainability* **2022**, *14*, 8612. [[CrossRef](#)]
9. Rizwan, A.M.; Dennis, L.Y.; Chunho, L. A review on the generation, determination and mitigation of urban heat island. *J. Environ. Sci.* **2008**, *20*, 120–128. [[CrossRef](#)] [[PubMed](#)]
10. Giridharan, R.; Emmanuel, R. The impact of urban compactness, comfort strategies and energy consumption on tropical urban heat island intensity: A review. *Sustain. Cities Soc.* **2018**, *40*, 677–687. [[CrossRef](#)]
11. Shishegar, N. Street Design and Urban Microclimate: Analyzing the Effects of Street Geometry and Orientation on Airflow and Solar Access in Urban Canyons. *J. Clean Energy Technol.* **2013**, *1*, 52–56. [[CrossRef](#)]
12. Eslamirad; Nasim; De Luca, F.; Lylykangas, K.S. The role of building morphology on pedestrian level comfort in Northern climate. In *Journal of Physics: Conference Series*; IOP Publishing: Bristol, UK, 2021; Volume 2042, p. 012053. [[CrossRef](#)]
13. Eslamirad; Nasim; De Luca, F.; Lylykangas, K.S.; Yahia, S.B. Data generative machine learning model for the assessment of outdoor thermal and wind comfort in a northern urban environment. *Front. Archit. Res.* **2023**, *12*, 541–555. [[CrossRef](#)]
14. Eslamirad; Nasim; Kolbadinejad, S.M.; Mahdavejad, M.; Mehranrad, M. Thermal comfort prediction by applying supervised machine learning in green sidewalks of Tehran. *Smart Sustain. Built Environ.* **2020**, *9*, 361–374. [[CrossRef](#)]
15. Rosenzweig, C.; Solecki, W.D.; Romero-Lankao, P.; Mehrotra, S.; Dhakal, S.; Ibrahim, S.A. (Eds.) *Climate Change and Cities: Second Assessment Report of the Urban Climate Change Research Network*; Cambridge University Press: Cambridge, UK, 2018. [[CrossRef](#)]
16. Martilli, A.; Krayerhoff, E.S.; Nazarian, N. Is the Urban Heat Island intensity relevant for heat mitigation studies? *Urban Clim.* **2020**, *31*, 100541. [[CrossRef](#)]
17. Kim, S.W.; Brown, R.D. Urban heat island (UHI) variations within a city boundary: A systematic literature review. *Renew. Sustain. Energy Rev.* **2021**, *148*, 111256. [[CrossRef](#)]
18. Wang, X.; Li, H.; Sodoudi, S. The effectiveness of cool and green roofs in mitigating urban heat island and improving human thermal comfort. *Build. Environ.* **2022**, *217*, 109082. [[CrossRef](#)]

19. Montávez, Juan, P.; Rodríguez, A.; Jiménez, J.I. A study of the urban heat island of Granada. *Int. J. Climatol. A J. R. Meteorol. Soc.* **2000**, *20*, 899–911. [[CrossRef](#)]
20. Wang, Y.; Berardi, U.; Akbari, H. Comparing the effects of urban heat island mitigation strategies for Toronto, Canada. *Energy Build.* **2016**, *114*, 2–19. [[CrossRef](#)]
21. Dionysia, K.; Lilli, K.; Gobakis, K.; Mavriaggiannaki, A.; Haddad, S.; Garshasbi, S.; Mohajer, H.R.H.; Paolini, R.; Vasilakopoulou, K.; Bartesaghi, C.; et al. Analyzing the Impact of Urban Planning and Building Typologies in Urban Heat Island Mitigation. *Buildings* **2022**, *12*, 537. [[CrossRef](#)]
22. Chao, X.; Chen, G.; Huang, Q.; Su, M.; Rong, Q.; Yue, W.; Haase, D. Can improving the spatial equity of urban green space mitigate the effect of urban heat islands? An empirical study. *Sci. Total Environ.* **2022**, *841*, 156687. [[CrossRef](#)]
23. Cortes, A.; Rejuso, A.J.; Santos, J.A.; Blanco, A. Evaluating mitigation strategies for urban heat island in mandaue city using envi-met. *J. Urban Manag.* **2022**, *11*, 97–106. [[CrossRef](#)]
24. Rajan, E.H.S.; Amirtham, L.R. Urban heat island intensity and evaluation of outdoor thermal comfort in Chennai, India. *Env. Dev Sustain.* **2021**, *23*, 16304–16324. [[CrossRef](#)]
25. Darbani, S.; Elham; Parapari, D.M.; Boland, J.; Sharifi, E. Impacts of urban form and urban heat island on the outdoor thermal comfort: A pilot study on Mashhad. *Int. J. Biometeorol. Vol. Int. J. Biometeorol.* **2021**, *65*, 1101–1117. [[CrossRef](#)] [[PubMed](#)]
26. Farhadi, H.; Faizi, M.; Sanaieian, H. Mitigating the urban heat island in a residential area in Tehran: Investigating the role of vegetation, materials, and orientation of buildings. *Sustain. Cities Soc.* **2019**, *46*, 101448. [[CrossRef](#)]
27. Arnfield, A. Street design and urban canyon solar access. *Energy Build.* **1990**, *14*, 117–131. [[CrossRef](#)]
28. van Esch, M.; Looman, R.; de Bruin-Hordijk, G. The effects of urban and building design parameters on solar access to the urban canyon and the potential for direct passive solar heating strategies. *Energy Build.* **2012**, *47*, 189–200. [[CrossRef](#)]
29. Steeneveld, G.J.; Koopmans, S.; Heusinkveld, B.G.; van Hove, L.W.A.; Holtslag, A.A.M. Quantifying urban heat island effects and human comfort for cities of variable size and urban morphology in The Netherlands. *J. Geophys. Res.* **2011**, *116*, D20129. [[CrossRef](#)]
30. Yahia, M.; Johansson, E. Influence of urban planning regulations on the microclimate in a hot dry climate: The example of Damascus, Syria. *J. Hous. Built Environ.* **2012**, *28*, 51–65. [[CrossRef](#)]
31. Battista, G.; de Lieto Vollaro, E.; Ocloñ, P.; de Lieto Vollaro, R. Effects of urban heat island mitigation strategies in an urban square: A numerical modelling and experimental investigation. *Energy Build.* **2023**, *282*, 112809. [[CrossRef](#)]
32. Ali-Toudert, F.; Mayer, H. Numerical study on the effects of aspect ratio and orientation of an urban street canyon on outdoor thermal comfort in hot and dry climate. *Build. Environ.* **2006**, *41*, 94–108. [[CrossRef](#)]
33. Eslamirad, N.; Sepúlveda, A.; De Luca, F.; Lylykangas, K.S. Evaluating outdoor thermal comfort using a mixed-method to improve the environmental quality of a university campus. *Energies* **2022**, *15*, 1577. [[CrossRef](#)]
34. Eslamirad; Nasim; De Luca, F.; Lylykangas, K.S.; Yahia, S.B.; Rasoulinezhad, M. Geoprocess of geospatial urban data in Tallinn, Estonia. *Data Brief* **2023**, *48*, 109172. [[CrossRef](#)]
35. Peel, M.C.; Finlayson, B.L.; McMahon, T.A. Updated world map of the Köppen-Geiger climate classification. *Hydrology and Earth System Sciences. Hydrol. Earth Syst. Sci.* **2007**, *11*, 1633–1644. [[CrossRef](#)]
36. Eslamirad, N. Geoprocess of Geospatial Urban Data in Tallinn, Estonia. Mendely Data, V3, 4 02 2023. Available online: <https://data.mendeley.com/drafts/2bm7kdf8gb> (accessed on 11 May 2023).
37. General Data of Tallinn. Available online: <https://www.tallinn.ee/en/statistika/general-data-tallinn> (accessed on 5 April 2023).
38. Jamei, E.; Rajagopalan, P.; Seyedmahmoudian, M.; Jamei, Y. Review on the impact of urban geometry and pedestrian level greening on outdoor thermal comfort. *Renew. Sustain. Energy Rev.* **2016**, *54*, 1002–1017. [[CrossRef](#)]
39. Cohen, P.; Potchter, O.; Matzarakis, A. Human thermal perception of Coastal Mediterranean outdoor urban environments. *Appl. Geogr.* **2013**, *37*, 1–10. [[CrossRef](#)]
40. Deb, C.; Ramachandraiah, A. The significance of Physiological Equivalent Temperature (PET) in outdoor thermal comfort studies. *Int. J. Eng. Sci. Technol.* **2010**, *2*, 2825–2828.
41. Moazzam, M.F.U.; Doh, Y.H.; Lee, B.G. Impact of urbanization on land surface temperature and surface urban heat island using optical remote sensing data: A case study of jeju island, republic of korea. *Build. Environ.* **2022**, *22*, 109368. [[CrossRef](#)]
42. Neto, A.F.; Bianchi, I.; Wurtz, F.; Delinchant, B. *Thermal Comfort Assessment*; ELECON, Electricity Consumption Analysis and Energy Efficiency: Gujarat, India, 2016. [[CrossRef](#)]
43. Giampaolletti, M.; Pistore, L.; Zapata-Lancaster, G.; Goycoolea, J.P.F.; Janakieska, M.M.; Gramatikov, K.; Kocaman, E.; Kuru, M.; Andreucci, M.; Calis, G.; et al. *RESTORE Regenerative Technologies for the Indoor Environment—Inspirational Guidelines for Practitioners*; ELECON, Electricity Consumption Analysis and Energy Efficiency: Gujarat, India, 2020.
44. Nazarian, N.; Acero, J.A.; Norford, L. Outdoor thermal comfort autonomy: Performance metrics for climate-conscious urban design. *Build. Environ.* **2019**, *155*, 145–160. [[CrossRef](#)]
45. Chakrabarty, S. Scoring and Analysis of Likert Scale: Few Approaches. *J. Knowl. Manag. Inf. Technol.* **2014**, *1*, 31–44.
46. Joshi, A.; Kale, S.; Chandel, S.; Pal, D. Likert Scale: Explored and Explained. *Br. J. Appl. Sci. Technol.* **2015**, *7*, 396–403. [[CrossRef](#)]

Disclaimer/Publisher’s Note: The statements, opinions and data contained in all publications are solely those of the individual author(s) and contributor(s) and not of MDPI and/or the editor(s). MDPI and/or the editor(s) disclaim responsibility for any injury to people or property resulting from any ideas, methods, instructions or products referred to in the content.